Available online at www.eccomasproceedia.org
Eccomas Proceedia COMPDYN (2021) 1583-1595

ECCOMAS
Proceedia

COMPDYN 2021
8th ECCOMAS Thematic Conference on
Computational Methods in Structural Dynamics and Earthquake Engineering
M. Papadrakakis, M. Fragiadakis (eds.)
Streamed from Athens, Greece, 28 - 30 June 2021

BASE VERSUS TOP ACTIVE CONTROL TO IMPROVE DYNAMIC AND SEISMIC PERFORMANCES OF RIGID BLOCKS

A. Di Egidio[1], A. Contento[2], and S. Pagliaro[3]

[1]University of L'Aquila - DICEAA
via G. Gronchi 19, 64100 L'Aquila - Italy
e-mail: angelo.diegidio@univaq.it

[2]University of L'Aquila - DICEAA
via G. Gronchi 19, 64100 L'Aquila - Italy
e-mail: alessandro.contento@univaq.it

[3]University of L'Aquila - DICEAA
via G. Gronchi 19, 64100 L'Aquila - Italy
e-mail: stefano.pagliaro@graduate.univaq.it

Abstract. *This paper compares the efficiency of two active control systems based on the same control algorithm in protecting rigid block-like structures from overturning. The control algorithm is the Pole Placement Method that is aimed at transforming the rest position of a rigid block into a stable equilibrium point. The two control systems differ in the position of the actuator driven by the active control algorithm. In the first case, the block is placed on a horizontally translating support that is connected to the ground by an actuator able to provide a controlled displacement. In the second case, a small mass able to run at the top of the block is driven by an actuator capable of applying a controlled displacement. This kind of protection system is commonly called Active Mass Damper. The effectiveness of the two control systems is analysed by comparing the overturning spectra that represent the amplitude of the harmonic excitation able to overturn the block versus its circular frequency. Several simulations have been conducted using different recorded earthquakes to evaluate the performances of the two control methods in the reduction of the rocking angle and the protection from the overturning of the block. The results show the excellent performance of both the considered control systems.*

Keywords: Rigid block-like structures, base active control, active mass damper, pole placement method, rocking motion, overturning.

ISSN:2623-3347 Published by Eccomas Proceedia.
Peer-review under responsibility of the organizing committee of COMPDYN 2021.
doi:10.7712/120121.8583.18635

1 INTRODUCTION

The protection of rigid block-like elements such as obelisks, statues, storage boxes, transformers, cabinets, and racks for both civil and industrial use is a challenging topic for civil engineers. The most common failure of such elements is the overturning caused by base excitation. Different techniques have been proposed to prevent such overturning. The majority of the researchers proposed protection techniques that are based on passive control systems.

For example, in [1, 2], the authors studied the effectiveness of base anchorages. Some papers investigated the efficiency of base isolated systems [3, 4, 5, 6, 7]. Several authors used mass-dampers that have been modeled either in the shape of a pendulum [8, 9, 10, 11] or as a single degree of freedom mass running on the top of the rigid block [12, 13, 14]. Some papers presented the coupling of rigid bodies with inerter devices [15, 16]. Lately, some researchers studied the use of semi-active anchorages [17, 18], and active control techniques [19, 20, 21] to increase the amplitude of base excitation required to topple a rigid block.

This paper compares the efficiency of two active control systems based on the same control algorithm in protecting rigid block-like structures from overturning. The control algorithm is the Pole Placement Method that is aimed at transforming the rest position of a rigid block into a stable equilibrium point. In fact, in the classical rocking equations of rigid blocks based on Housners model [22], the rest position is not an equilibrium point. The two control systems differ in the position of the actuator driven by the active control algorithm. In the first control system, the block is placed on a horizontally translating support. Such support has a mass that is negligible compared to the mass of the block and it is connected to the ground by an actuator able to provide a controlled displacement. This protection system was already studied in [20]. In the second control system, a small mass able to run at the top of the block is driven by an actuator capable of applying a controlled displacement. This protection system is commonly called Active Mass Damper (AMD).

For both methods, the linearized rocking equations are used to derive the control laws. The optimal coefficients of the control laws are selected assuming the overshoot as the key parameter. Both the control systems exhibit a low sensitivity to the geometrical characteristics of the rigid block so that the same optimized control coefficients can be used for a wide class of rigid blocks. The robustness of the two control systems is also investigated by considering the limitations of the control forces and different sampling and delay times.

The effectiveness of the two control systems is analyzed by comparing the overturning spectra that are obtained with and without control. Such overturning spectra provide the amplitude of the harmonic excitation able to overturn the block versus its circular frequency. Several simulations have also been conducted using different recorded earthquakes to evaluate the performances of the two control methods in the reduction of the rocking angle and the protection from the overturning of the block under seismic excitation.

The results show the excellent performance of both the considered control systems. Consequently, since the performances of the control systems are comparable for all the working conditions considered, the choice between the two methods is dictated by the technical and technological aspects of each specific application.

2 ACTIVE CONTROL METHODS

In both the control methods the mechanical system is a rigid block in the shape of a parallelepiped with a height $2h$ and a base $2b$ (Fig. 1). The base dimension orthogonal to the rocking plane has unitary length. The mass of the block is $M = \rho \times 2b \times 2h \times 1.0$, where the mass den-

sity $\rho = 1800\mathrm{kg/m^3}$. The block cannot slide, so its motion is described by only the Lagrangian parameter $\theta(t)$ that is the rocking angle. In the first control method, the block is placed on a horizontally translating support. Such support has a mass that is negligible compared to the mass of the block and it is connected to the ground by an actuator able to provide the controlled displacement $u^B(t)$ (Fig. 1a). In the second control scheme, a small mass m, able to run at the top of the block, is driven by an actuator capable of applying the controlled displacement $u^T(t)$ (Fig. 1b).

The control algorithm used in this paper is the Pole Placement Method (PPM) that is aimed at transforming the rest position of a rigid block into a stable equilibrium point. It is worth observing that, the two rocking equations describing the motion around the two base pivots of a stand-alone rigid block, do not admit the rest position ($\theta(t) = 0$) as an equilibrium point. The PPM algorithm makes the rest position a stable equilibrium point in both the rocking equations.

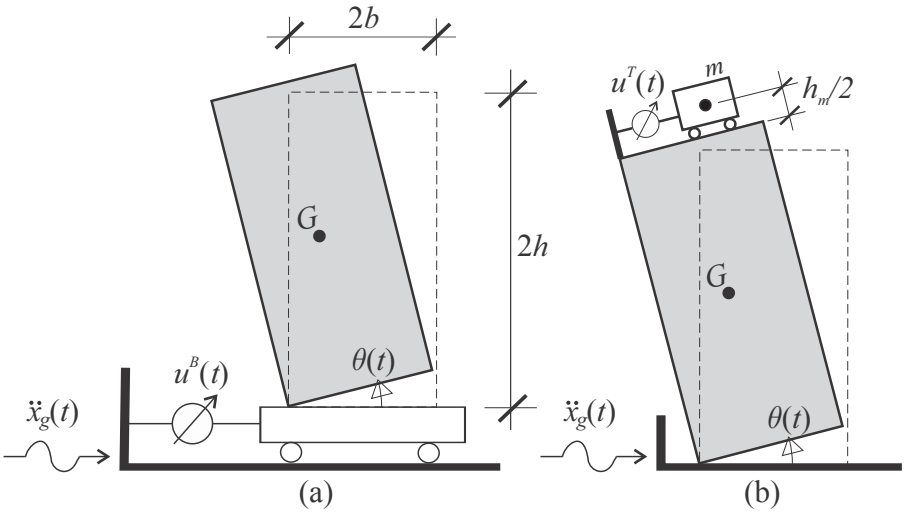

Figure 1: Active control systems: (a) Base Active Control (BAC); (b) Top Active Control (TAC) or active mass damper.

2.1 Base active control system

Since the active control system applied to the base of the rigid block and based on the Pole Placement Method was already studied in [20], in this subsection only the main governing equations are reported. The system shown in Fig. 1a can be described by the same equations of a stand-alone block with an additional term due to the control device. The control displacement $u^B(t)$ applies an acceleration $\ddot{u}^B(t)$ at the base of the block that works as the external excitation. Hence, it appears in the equations of motion as a contribution added to external acceleration $\ddot{x}_g$. The equations of motion read

$$\begin{aligned}
&\left(J_G + MR^2\right)\ddot{\theta}(t) + gMR\sin\left(\alpha_{cr} - \theta(t)\right) - MR\cos\left(\alpha_{cr} - \theta(t)\right)\left(\ddot{x}_g(t) + \ddot{u}^B(t)\right) = 0 \\
&\left(J_G + MR^2\right)\ddot{\theta}(t) - gMR\sin\left(\alpha_{cr} + \theta(t)\right) - MR\cos\left(\alpha_{cr} + \theta(t)\right)\left(\ddot{x}_g(t) + \ddot{u}^B(t)\right) = 0
\end{aligned} \tag{1}$$

where g is the gravity acceleration; J_G is the polar momentum evaluated with respect to the mass centre G; α_{cr} is the value of $\theta(t)$ in which the vertical projection of the mass centre G passes through the base rocking corner; R is the distance between the mass centre G and the base rocking corner.

The control algorithm is obtained by linearising the equations of rocking motion with respect to $\theta(t)$. This assumption leads to an excellent approximation in the case where $\theta(t)$ is very small. This fact occurs in sufficiently tall blocks where θ has to be smaller than the critical angle α_{cr}.

The Pole Placement Method has two main objectives: (i) to vanish the external excitation at each instant and (ii) to make the rest position of the block a stable point. The first objective is achieved by providing a control force opposite to the external one to the system. For the second objective, the rest position of the block can be considered a stable point if the Jacobian matrix is modified in such a way that the eigenvalues have negative real part. The control law $\ddot{u}^B(t)$, representing the control acceleration that the actuator has to apply to the system at each time t reads

$$\ddot{u}^B(t) = \pm g\alpha_{cr} - \ddot{x}_g(t) - \frac{1}{4}\left(4 + q_{22}^2\right)\vartheta(t) - \frac{g}{\omega_o}q_{22}\dot{\vartheta}(t) \tag{2}$$

where q_{22} is a control coefficient that has to be determined. The sign $(-)$ refers to the rocking motion around the left corner, whereas the sign $(+)$ refers to rocking motion around the right corner.

2.2 Active mass damper system

The equations of motion of the controlled system in Fig. 1b are obtained via a Lagrangian approach

$$\begin{gathered}
0.25\,[\theta''(t)(4b^2(m+M) + m(4u(t)(2b+u(t)) + h_m^2 + 8hh_m) + 4h^2(4m+M)) + \\
4m(2b\dot{\theta}(t)\dot{u}(t) + u(t)\left(g\cos(\theta(t)) + 2\dot{\theta}(t)\dot{u}(t)\right) - 2h\ddot{u}(t)) + \\
4\ddot{x}_g(t)(-\sin(\theta(t))(b(m+M) + mu(t)) - h(2m+M)\cos(\theta(t))) - \\
2mh_m(g\sin(\theta(t)) + \ddot{u}(t) + \cos(\theta(t))\ddot{x}_g(t))] + \\
bg(m+M)\cos(\theta(t)) - gh(2m+M)\sin(\theta(t)) + J_G\ddot{\theta}(t) = 0 \\
0.25\,[\ddot{\theta}(t)(4b^2(m+M) + m(4u(t)(u(t)-2b) + h_m^2 + 8hh_m) + 4h^2(4m+M)) - \\
2m(4b\dot{\theta}(t)\dot{u}(t) + gh_m\sin(\theta(t)) - 2gu(t)\cos(\theta(t)) + (h_m+4h)\,\ddot{u}(t) - \\
4u(t)\dot{\theta}(t)\dot{u}(t)) + 2\ddot{x}_g(t)(2\sin(\theta(t))(b(m+M) - mu(t)) - \\
(2h(2m+M) + mh_m)\cos(\theta(t)))] - \\
bg(m+M)\cos(\theta(t)) - gh(2m+M)\sin(\theta(t)) + J_G\ddot{\theta}(t) = 0
\end{gathered} \tag{3}$$

where $h_m/2$ is the vertical distance between the centre of the small mass m and the top of the block (see Fig. 1b.) Also in this case the control algorithm is obtained by linearising the equations of rocking motion with respect to the variables $\theta(t)$ as

$$\dot{\mathbf{Z}}(t) = \mathbf{A}_1(t)\mathbf{Z}(t) + \mathbf{A}_2 + \mathbf{A}_3\ddot{x}_g(t) + \mathbf{A}_4\ddot{u}^T(t) \tag{4}$$

where $\mathbf{Z}(t) = \left\{ \begin{array}{cc} \theta(t) & \dot{\vartheta}(t) \end{array} \right\}^T$ is the state variables vector and the matrices $\mathbf{A}_1$, $\mathbf{A}_2$, $\mathbf{A}_3$, and $\mathbf{A}_4$ read

$$\begin{gathered}
\mathbf{A}_1(t) = \left[\begin{array}{cc} 0 & 1 \\ \omega_0^2 & \mp\frac{2bm}{J_{A,B}}\dot{u}^T(t) \end{array} \right]; \quad \mathbf{A}_2 = \left\{ \begin{array}{c} 0 \\ \mp\frac{bg(m+M)}{J_{A,B}} \end{array} \right\} \\
\mathbf{A}_3 = \left\{ \begin{array}{c} 0 \\ \frac{\omega_0^2}{g} \end{array} \right\}; \quad \mathbf{A}_4 = \left\{ \begin{array}{c} 0 \\ \frac{\omega_0^2}{g} - \frac{hM}{J_{A,B}} \end{array} \right\}
\end{gathered} \tag{5}$$

where $\omega_0^2 = (hM + (2h + h_m/2)m)\, g/J_{A,B}$ is the linear frequency associated to the motion of the block and $J_A = J_B$ is the total polar momentum evaluated with respect to one of the base rocking corners. The following control law is assumed:

$$\mathbf{A}_4 \ddot{u}^T(t) = -\mathbf{A}_2 - \mathbf{A}_3 \ddot{x}_g(t) - \mathbf{Q}(t)\mathbf{Z}(t) \tag{6}$$

where $\mathbf{Q}(t)$ is a weighting matrix

$$\mathbf{Q}(t) = \begin{bmatrix} 0 & 1 \\ \omega_0^2 q_{12} & \omega_0 q_{22} \mp \frac{2bm}{J_{A,B}} \dot{u}^T(t) \end{bmatrix} \tag{7}$$

By introducing Eq. 6 into the linearised equations Eq. 4, the linearised controlled system becomes

$$\dot{\mathbf{Z}}(t) = (\mathbf{A}_1(t) - \mathbf{Q}(t))\, \mathbf{Z}(t) \tag{8}$$

where the Jacobian matrix of the controlled system $\mathbf{A}_1(t) - \mathbf{Q}(t)$ does not depend on time. The linearised system Eq. 8 admits the rest position $\theta(t) = 0$ as stable equilibrium point if the eigenvalues of the linearised Jacobian matrix are real, negative, and coincident. This fact occurs for the control coefficient $q_{12} = 1/4(4 + q_{22}^2)$.

By expanding Eq. 6, it is possible to observe that the control displacement $u^T(t)$ has to satisfy the following differential equation:

$$\ddot{u}^T(t) \mp c_u(\dot{\theta})\dot{u}^T(t) \mp c_0 + c_g(\ddot{x}_g) + c_\theta(\theta) + c_{\dot{\theta}}(\dot{\theta}) = 0 \tag{9}$$

where the coefficients in the equation are

$$\begin{gathered} c_u(\dot{\theta}) = \tfrac{2bmg}{J_{A,B} - hMg}\dot{\theta}; \quad c_0 = \tfrac{bg^2(M+m)}{J_{A,B} - hMg}; \quad c_g(\ddot{x}_g) = \tfrac{J_{A,B}\omega_0^2}{J_{A,B} - hMg}\ddot{x}_g \\ c_\theta(\theta) = \tfrac{1}{4}\tfrac{J_{A,B} g \omega_0^2}{J_{A,B} - hMg}(4 - q_{22}^2)\theta; \quad c_{\dot{\theta}}(\dot{\theta}) = \tfrac{1}{4}\tfrac{J_{A,B} g \omega_0}{J_{A,B} - hMg} q_{22}\dot{\theta} \end{gathered} \tag{10}$$

2.3 Ideal and real controlled system

The real working conditions of the controlled system differ from the ideal case because (i) the control accelerations $\ddot{u}^{B,T}$ have to be limited to a threshold value that depend on the characteristics of the actuator, (ii) the control device applies the accelerations $\ddot{u}^{B,T}$ with a delay that depends on the characteristics of the control system, and (iii) the control algorithm is obtained from the linearised equations of motion, hence it works sufficiently well with the nonlinear mechanical system if the smallness of the rocking angle θ can be considered a valid approximation.

It is considered that the actuators can reach the maximum acceleration $\ddot{u}^B_{max} = 0.2g$ and $\ddot{u}^T_{max} = 2.0g$, respectively for the base and the top active control system. Therefore, by taking the moving mass of Fig. 1b $m = \gamma M$, with $\gamma = 0.1$, it follows that the maximum control forces $F^B_{max} = M0.2g$ and $F^T_{max} = m2.0g = \gamma M 2.0g$ are equal. In the simulations performed in the paper, it is always considered this threshold value of the controlled accelerations.

As it is known, real control systems suffer of time-delays between the real time and the application of the control displacement. One of the delays is the so-called sampling time δt_c, which measures the time-step between two successive data acquisitions of the state variables necessary to evaluate the control displacement. The other type of delay is the time-delay δt_d, which is related to the speed of the control system and of the actuator to evaluate and to apply

the control displacement to the system. An analysis to evaluate the robustness of the control systems to a variation of the time-delays is performed below.

Both active control systems depend only on the coefficient q_{22} (Eq. 2 and Eqs. 9-10). The search of the optimal value of such coefficient can be usually performed in terms of step response of the system ([23]). In a rigid block system the step input cannot assume any value because the block overturns over a threshold of the base acceleration. Hence, a small constant base acceleration, capable of uplifting the block but not sufficient to overturn it, is considered. The efficiency of the control system can be measured by evaluating the so called *overshoot*. Under a step excitation, the block uplifts, reaches the overshoot, that is the maximum rocking amplitude, and comes back to the rest position, thanks to the control apparatus. A parametric analysis is performed in order to evaluate the overshoot as a function of the sole control coefficient q_{22}, in both the considered control systems. Such parametric analysis provide the same value of the control coefficient $q_{22} = 7$ for both control systems.

3 UPLIFT AND IMPACT CONDITIONS

In order to correctly describe the behaviour of the system, the knowledge of the transition conditions among the different possible phases of motion is needed. The system at hand presents two transition conditions: uplift and impact.

The uplift condition provides the minimum base acceleration a_{up} capable of uplifting the block. It is assumed that the control system works after the beginning of the rocking motion. The minimum value of the horizontal acceleration able to uplift the block can be obtained from the balance between the resisting moment (due to the weight of the block) and the overturning moment (due to the inertial forces).

During the rocking motion, when the rotation $\theta(t)$ approaches to zero, an impact between the block and the support occurs. Consequently, the pivot of the rocking motion changes and it is necessary to evaluate the angular velocity of the block after the impact. Post-impact conditions of the rocking motion can be found assuming that the impact happens instantly, the block position remains unchanged, and the conservation of the angular momentum is imposed.

3.1 Base Active Control system

Since the control system works only after the beginning of rocking motion, the uplift and impact conditions are the same as those of a stand-alone rigid block. The uplift condition reads

$$|a_{up}| \geq \frac{g}{\lambda} \tag{11}$$

where $\lambda = h/b$ is the slenderness of the block. An uplift occurs around the left (right) base corner when $a_{up} > 0$ ($a_{up} < 0$).

The impact condition provides the following restitution coefficient

$$\mu = \frac{\dot{\vartheta}^+}{\dot{\vartheta}^-} = \frac{(J_O - 2bS_y)}{J_O} \tag{12}$$

where J_O is the polar inertia of the block with respect one of the two base corners; $S_y = \pm Mb$ (sign minus in case of re-uplift around the left base corner, sign plus in case of re-uplift around the right corner) is the static moment of the block with respect to a vertical axis passing through one of the two base corners and superscript $(\cdot)^-$ and superscript $(\cdot)^+$ denote pre- and post-impact quantities respectively.

3.2 Top Active Control system

The acceleration able to uplift the system can be found from the balance between the resisting and the overturning momenta as

$$|a_{up}| \geq \frac{(M+m)bg}{Mh + m\left(2h + \frac{h_m}{2}\right)} \tag{13}$$

An uplift occurs around the left (right) base corner when $a_{up} > 0$ ($a_{up} < 0$). By imposing the conservation of the angular momentum before and after an impact, both evaluated respect to the re-uplifting corner, the following restitution coefficient is obtained:

$$\mu = \frac{\dot{\vartheta}^+}{\dot{\vartheta}^-} = \frac{4\left(J_O - 2bS_y + m\left(-b^2 + 4h^2 + u(t)^2\right)\right) + mh_m^2 + 8hmh_m}{4\left(J_O + m\left(b^2 + 2bu(t) + 4h^2 + u(t)^2\right)\right) + mh_m^2 + 8hmh_m} \tag{14}$$

It is worth observing that, if $m = 0$ the uplift and the impact conditions given by Eq. 13 and Eq. 14 becomes the same as those of a stand-alone rigid block.

4 PARAMETRIC ANALYSIS

4.1 Harmonic excitation

An harmonic base excitation is first considered. It reads

$$\ddot{x}_g(t) = A_s \sin(\Omega t) \qquad 0 \leq t \leq t_{\max} \tag{15}$$

where $\Omega = 2\pi/T_s$ is the circular frequency of the excitation, T_s is the period of the harmonic cycle, A_s is its amplitude, and $t_{\max} = 10$s is the maximum time used in the numerical integrations. The assessment of the efficiency of the two control algorithms in protecting the block from the overturning is performed by comparing the results obtained with those of the uncontrolled system. A parametric analysis is performed to obtain overturning spectra, where the overturning amplitude A_s of the excitation is plotted versus the frequency Ω. The single overturning spectrum is obtained for blocks with fixed base $2b$, fixed slenderness λ, and fixed upper limit of the control forces $F^B_{max} = F^T_{max}$ (as explained in Subsection 2.3).

The overturning spectra referring to two blocks with different geometrical characteristics are shown in Fig. 2. Specifically, the spectra in the first row of the figure refer to a block with $2b = 0.4$ m and $\lambda = 5$, whereas the spectra in the second row refer to a block with $2b = 0.6$ m and $\lambda = 7$. Figure 2a shows the spectra of both the blocks obtained for three different couples of time delays and where the Base Active Control (BAC) is used. As can be observed, the spectra obtained for different time-delays are very close to each other. This means that the BAC system manifest a good robustness to time-delays. In Figure 2b the spectra of both blocks with the Top Active Control (TAC) and different time-delays are reported. The results show that the TAC system is more sensible to time-delays than the BAC system. This means that the TAC does not manifest a good robustness to time-delays. However, when the time-delays increase (from the dashed curve to the dotted curve), the distance among the spectra reduces.

Finally, the comparison among overturning spectra with the BAC system, the TAC system, and with No Active Control (NAC) are shown in Fig. 2c. These spectra refer to a fixed couple of time-delays ($\delta t_c = 0.1s$ and $\delta t_d = 0.05s$), that refer to a control apparatus of mean characteristics as in [17] and [18]. As can be observed, both the control systems exhibit a better performance than the case without active control. Nevertheless, the TAC system assures the

best performances in reducing the overturning of the block, since for each frequency Ω of the harmonic excitation the overturning of the block occurs for higher amplitude A_s of the excitation.

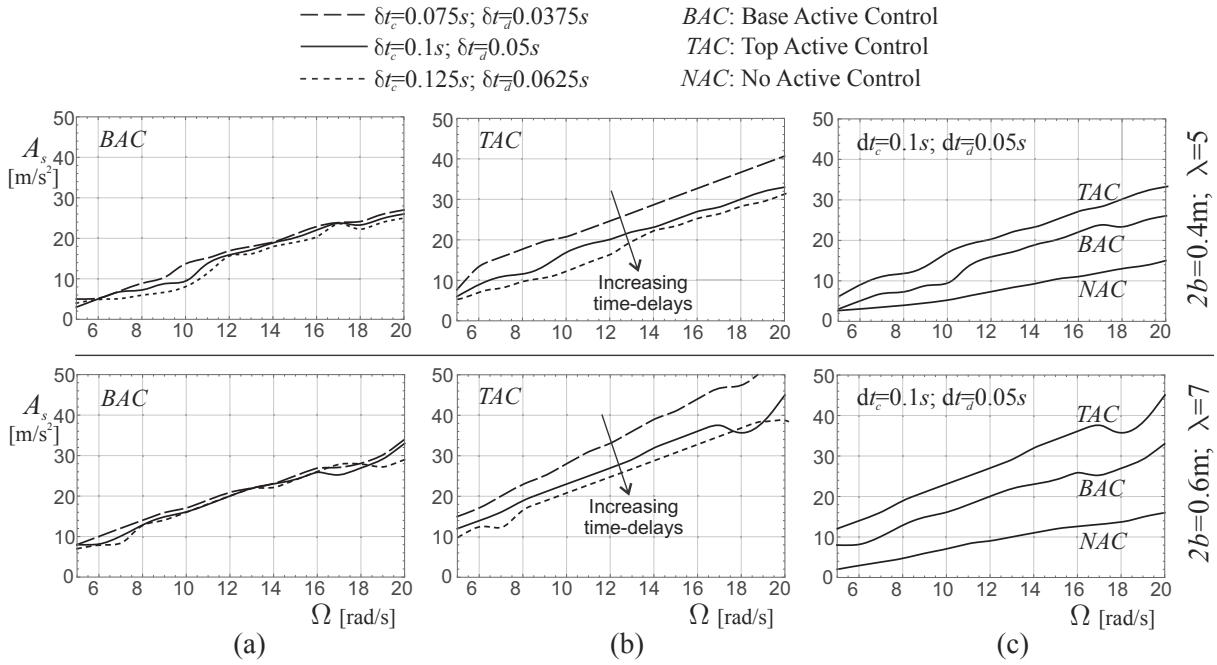

Figure 2: Overturning spectra: (a) spectra of the Base Active Control (BAC) system obtained for different time-delays; (b) spectra of the Top Active Control (TAC) system obtained for different time-delays; (c) comparison among spectra for fixed time-delays ($F^B_{max} = F^T_{max}$, $F^B_{max} = 0.2Mg$, $F^T_{max} = 2.0mg$, $m = \gamma M$, $\gamma = 0.1$).

4.2 Seismic excitation

Two earthquake records are used as seismic input. The earthquake records are

- Kobe, Takarazuka-000 station, ground motion recorded during the 1995 Japan earthquake;
- Parkfield, CO2-065 ground motion recorded during the California earthquake 1966.

Figure 3 shows the time-histories (left graphs) and the pseudo-acceleration elastic spectra (right graphs) of the two earthquake records. The results of the parametric analyses are shown by means of rocking maps that represent the contour plots (for a single seismic record) of the maximum rocking angle in the parameter plane $(2b-\lambda)$. The regions where the block overturns ($i.e.$, where the maximum rocking angle is $\theta_{max} = \pi/2$) are colored in dark grey; the regions where the block does not overturn are colored in light grey, and the contour levels represent the maximum values of $\theta(t)$. For each earthquake, the rocking maps of the two control systems and the map obtained without active control are compared. In the analysis, the sampling time and time-delay are assumed as $\delta t_c = 0.1s$ $\delta t_d = 0.05s$, respectively, as in ([17] and [18]).

In Fig. 4 the rocking maps are organized in matrix form. Along the two columns there are the maps of the earthquake records (Kobe and Pacoima), whereas the rows refer to NAC, BAC, and TAC. As can be observed, the active control systems drastically reduce the overturning regions (dark grey regions) with respect to the case without active control. However, the TAC appears to

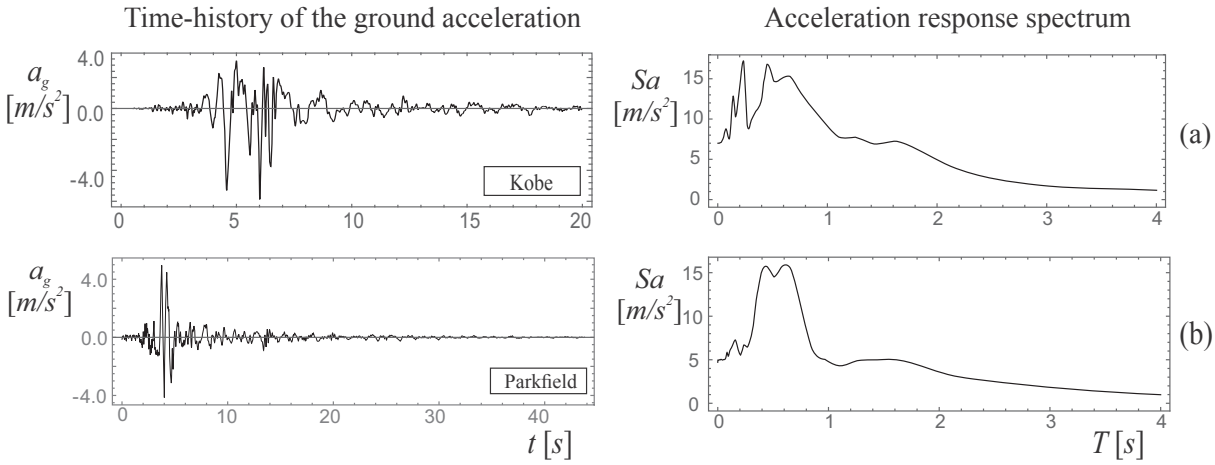

Figure 3: Time-histories (left graphs) and pseudo-acceleration elastic spectra (right graphs) of the earthquakes analysed: (a) Kobe; (b) Parkfield.

be able to extend the safety region (i.e., the regions where no overturning occurs) to the whole parameter $(2b - \lambda)$ plane. In fact, the BAC is not able to protect the block from overturning in the whole parameter plane under Kobe earthquake, as done by the TAC (see maps of the second row in Fig. 4).

Fig. 5 shows sections of the rocking maps that help to understand the efficiency of the control systems in reducing θ_{max}. The sections are identified by paths I and II in Fig. 4. Specifically, Fig. 5a shows the two section along path I, referring to Kobe earthquake, obtained for the Base and the Top Active Control systems. Instead, Fig. 5b shows the two section along path II, referring to Parkfield earthquake, obtained for the BAC and the TAC systems. As can be can be observed, the use of the TAC system generally leads to values of θ_{max} smaller than those obtained by using the BAC system.

5 CONCLUSIONS

The performances in protecting rigid blocks from the overturning of two different active control systems, both based on the same active control algorithm (i.e., the Pole Placement Method), were investigated and compared. In the first control system, the block is placed on a horizontally translating support that is connected to the ground by an actuator able to provide a controlled displacement. In the second control system, a small mass able to run on the top of the block is driven by an actuator capable of applying a controlled displacement. The control algorithm based on the Pole Placement Method acts both vanishing the external excitation at each instant by imposing a control force opposite to the external one and making the rest position of the block a stable point by suitably modifying the Jacobian matrix of the system and its eigenvalues. A preliminary analysis that considers the overshoot as key parameter was performed to evaluate the optimal coefficients of the control law for the two systems. The optimal value of such coefficients weakly depends on the parameters characterizing the mechanical system and is the same for the two different control systems.

The effectiveness of the two control systems was analysed by comparing the overturning spectra that represent the amplitude of the harmonic excitation able to overturn the block versus its circular frequency. Results showed that both control systems significanlty improve the behaviour of the rigid block with respect to the case without control. Nevertheless, if on the

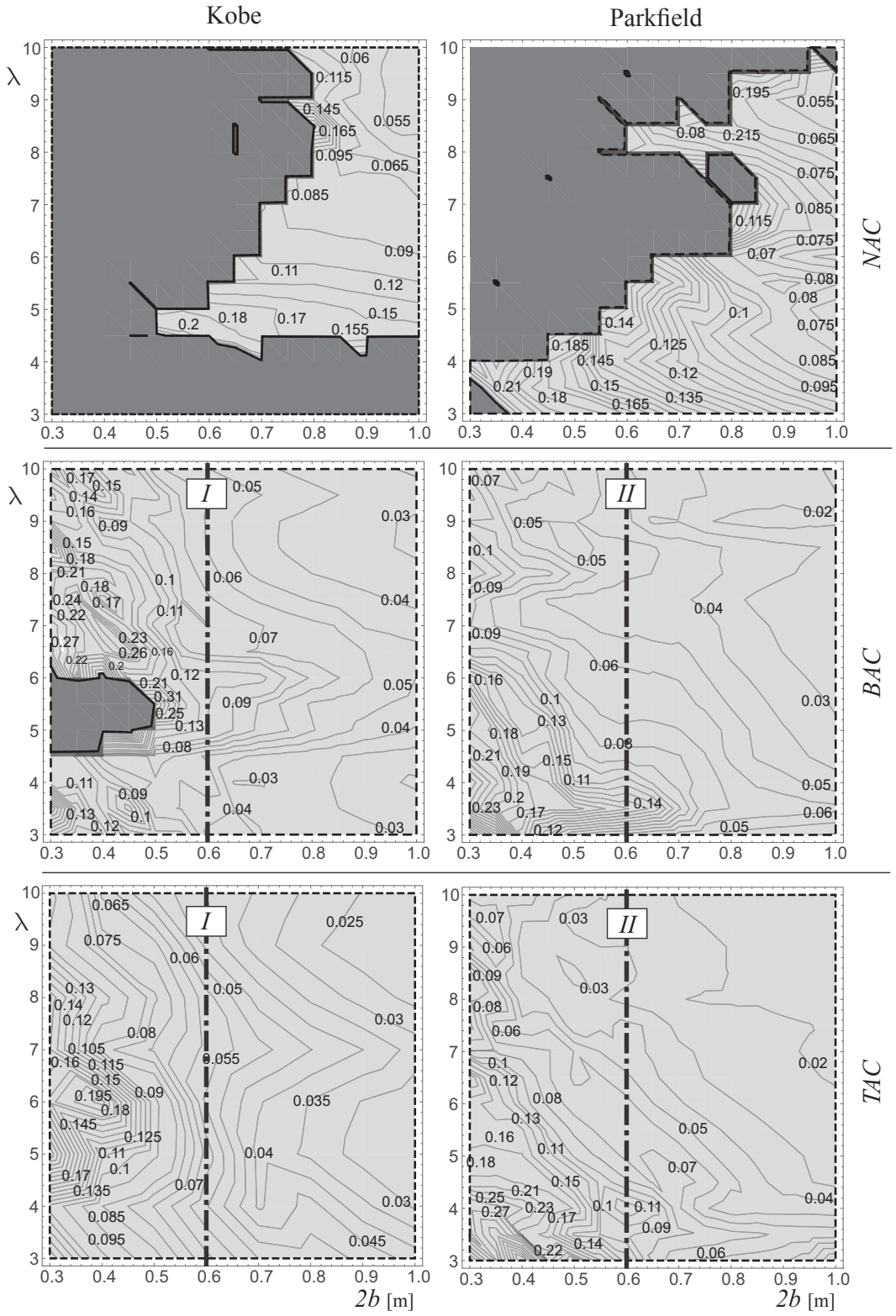

Figure 4: Rocking maps for two different earthquakes (Kobe e Parkfield) and three different configurations: No Active Control (NAC), Base Active Control (BAC), and Top Active Control (TAC).

one hand, the Top Active Control system manifests better performances than the Base Active Control system, on the other hand, this last exhibits an higher robustness to time-delays. Other

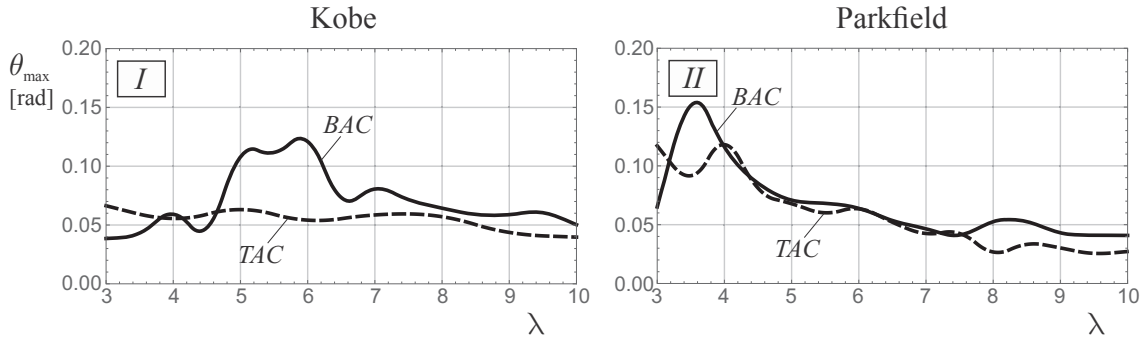

Figure 5: Sections of rocking maps for two different earthquakes (Kobe e Parkfield) and two different configurations: Base Active Control (BAC), and Top Active Control (TAC); ($2b = 0.6$ m).

simulations were also conducted using two recorded earthquakes to evaluate the performances of the control methods in the reduction of the rocking angle and the protection from the overturning of the block. The results showed the excellent performance of both the considered control systems. To conclude, since the performances of the control systems are comparable for all the working conditions considered, the choice between the two methods is dictated by the technical and technological aspects of each specific application.

References

[1] N. Makris and J. Zhang. Rocking response of anchored blocks under pulse-type motions. *Journal of Engineering Mechanics*, 127(5):484–493, 2001.

[2] E.G. Dimitrakopoulos and M.J. DeJong. Overturning of retrofitted rocking structures under pulse-type excitations. *Journal of Engineering Mechanics*, 138:963–972, 2012.

[3] A. Di Egidio and A. Contento. Base isolation of sliding-rocking non-symmetyric rigid blocks subjected to impulsive and seismic excitations. *Engineering Structures*, 31:2723–2734, 2009.

[4] A. Di Egidio and A. Contento. Seismic response of a non-symmetric rigid block on a constrained oscillating base. *Engineering Structures*, 32:3028–3039, 2010.

[5] A. Contento and A. Di Egidio. On the use of base isolation for the protection of rigid bodies placed on a multi-storey frame under seismic excitation. *Engineering Structures*, 62-63:1–10, 2014.

[6] I. Caliò and M. Marletta. Passive control of the seismic response of art objects. *Engineering Structures*, 25:1009–1018, 2003.

[7] M.F. Vassiliou and N. Makris. Analysis of the rocking response of rigid blocks standing free on a seismically isolated base. *Earthquake engineering and structural dynamics*, 41(2):177–196, 2012.

[8] L. Collini, R. Garziera, K. Riabova, M. Munitsyna, and A. Tasora. Oscillations control of rocking-block-type buildings by the addition of a tuned pendulum. *Shock and Vibration*, 2016:Article ID 8570538, 2016.

[9] P. Brzeski, T. Kapitaniak, and P. Perlikowski. The use of tuned mass absorber to prevent overturning of the rigid block during earthquake. *International Journal of Structural Stability and Dynamics*, 6(10):Article ID 1550075, 2016.

[10] A. de Leo, G. Simoneschi, C. Fabrizio, and A. Di Egidio. On the use of a pendulum as mass damper to control the rocking motion of a non-symmetric rigid block. *Meccanica*, 51:2727–2740, 2016.

[11] A. Di Egidio, R. Alaggio, A. Aloisio, A.M. de Leo, A. Contento, and M. Tursini. Analytical and experimental investigation into the effectiveness of a pendulum dynamic absorber to protect rigid blocks from overturning. *Int. Journal of Non-Linear Mechanics*, 115:1–10, 2019.

[12] G. Simoneschi, A. de Leo, and A. Di Egidio. Effectiveness of oscillating mass damper system in the protection of rigid blocks under impulsive excitation. *Engineering Structures*, 137:285–295, 2017.

[13] G. Simoneschi, A. Geniola, A. de Leo, and A. Di Egidio. On the seismic performances of rigid blocks coupled with an oscillating mass working as tmd. *Earthquake Engineering and Structural Dynamics*, 46:1453–1469, 2017.

[14] A. Di Egidio, A. de Leo, and G. Simoneschi. Effectiveness of mass-damper dynamic absorber on rocking block under one-sine pulse ground motion. *International Limits of Non-Linear Mechanics*, 98:154–162, 2018.

[15] R. Thiers-Moggia and M. Mlaga-Chuquitaype. Seismic protection of rocking structures with inerters. *Earthquake Engineering and Structural Dynamics*, 48(5):528–457, 2019.

[16] A. Di Egidio, S. Pagliaro, and C. Fabrizio. Combined use of rocking wall and inerters to improve the seismic response of frame structures. *Journal of Engineering Mechanics*, 2021 (accepted, in press).

[17] R. Ceravolo, M.L. Pecorelli, and L. Zanotti Fragonara. Semi-active control of the rocking motion of monolithic art objects. *Journal of Sound and Vibration*, 374:1–16, 2016.

[18] R. Ceravolo, M.L. Pecorelli, and L. Zanotti Fragonara. Comparison of semi-active control strategies for rocking objects under pulse and harmonic excitations. *Mechanical Systems and Signal Processing*, 90:175–188, 2017.

[19] A. Di Egidio, G. Simoneschi, C. Olivieri, and A.M. de Leo. Protection of slender rigid blocks from the overturning by using an active control system. In *Proceedings of the XXIII Conference The Italian Association of Theoretical and Applied Mechanics*, 2014.

[20] G. Simoneschi, C. Olivieri, A.M. de Leo, and A. Di Egidio. Pole placement method to control the rocking motion of rigid blocks. *Engineering Structures*, 167:39–47, 2018.

[21] A. Di Egidio, C. Olivieri, and A.M. de Leo. Protection from overturning of rigid block-like objects with linear quadratic regulator active control. *Structural Control and Health Monitoring*, 27, 2020.

[22] G.W. Housner. The behavior of inverted pendulum structures during earthquakes. *Bulletin of the Seismological Society of America*, 53(2):404417, 1963.

[23] R.C. Dorf and R.H. Bishop. *Modern control system*, 2008.